JACS
JOURNAL OF THE AMERICAN CHEMICAL SOCIETY
pubs.acs.org/JACS
Article

DNA Dendron Tagging as a Universal Way to Deliver Proteins to Cells

Published as part of Journal of the American Chemical Society special issue "Nano-Biomaterials for Tissue Interactions and Therapeutics".

Kathleen H. Ngo, Max E. Distler, Michael Evangelopoulos, Tonatiuh A. Ocampo, Yinglun Ma, Andrew J. Minorik, and Chad A. Mirkin*

Cite This: J. Am. Chem. Soc. 2025, 147, 2129–2136

ABSTRACT: The use of proteins as intracellular probes and therapeutic tools is often limited by poor intracellular delivery. One approach to enabling intracellular protein delivery is to transform proteins into spherical nucleic acid (proSNA) nanoconstructs, with surfaces chemically modified with a dense shell of radially oriented DNA that can engage with cell-surface receptors that facilitate endocytosis. However, proteins often have a limited number of available reactive surface residues for DNA conjugation such that the extent of DNA loading and cellular uptake is restricted. Indeed, DNA surface density and sequence have been correlated with scavenger-receptor engagement, the first step of cellular internalization. Here, we report how branched DNA dendrons with dibenzocyclooctyne groups and proteins genetically engineered to include the noncanonical amino acid azido-phenylalanine for click chemistry can be used to synthesize hybrid DNA dendron-protein architectures that exhibit outstanding cellular internalization properties, without the need for extensive surface modification. In a head-to-head comparison, protein−DNA dendron structures (where DNA is concentrated in a local area) are taken up by cells more rapidly and to a greater extent than proSNAs (where the DNA is evenly distributed). Also, protein-G-rich dendron structures show enhanced uptake compared to protein-T-rich dendron structures, highlighting the importance of oligonucleotide sequence on nanoconjugate uptake. Finally, a generalizable method for chemically tagging proteins with dendrons that does not require mutagenesis is described. When a range of proteins, spanning 42 to 464 kDa, were modified through surface lysines with this method, a significant increase in their cellular uptake (up to 17-fold) compared to proteins that are not coupled to a DNA dendron was observed.

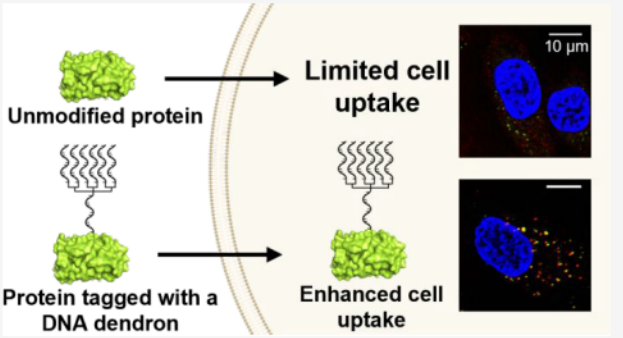

INTRODUCTION

Proteins possess several properties that make them desirable as intracellular therapeutics, including their biocompatibility, role in many cellular functions, and high target specificity. Indeed, they are promising materials for protein replacement therapies.[1−4] Despite this potential, current protein therapeutics can only access membrane-bound or extracellular targets, leaving intracellular targets relatively underexplored.[5−8] Due to their large sizes and hydrophilic surfaces, compared to small molecule drugs, proteins do not typically penetrate cell membranes. To overcome this issue, positively charged cell-penetrating peptides have been attached to proteins to facilitate their interaction with cell membranes and thus enhance their uptake in vitro.[9−14] Alternatively, certain proteins can be transformed into spherical nucleic acids (proSNAs) by modifying their periphery and surface accessible lysine residues with a dense layer of DNA.[15−19] The resulting oligonucleotide shell is recognized by class-A scavenger receptors, which facilitates their cellular uptake.[20−24] However, functionalizing the entire outer surface of a protein with oligonucleotides can compromise its function and, consequently, therapeutic or diagnostic use. Moreover, certain proteins lack the requisite number of surface functional groups to allow the generation of structures with a dense enough DNA shell to realize SNA-like properties (e.g., cellular uptake and resistance to degradation).[17,25−27]

DNA dendrons, molecular nanostructures consisting of a DNA stem and a controlled number of DNA branches, can potentially overcome this limitation. Such dendrons exhibit

Received: November 15, 2024
Revised: December 10, 2024
Accepted: December 13, 2024
Published: December 30, 2024

https://doi.org/10.1021/jacs.4c16205
J. Am. Chem. Soc. 2025, 147, 2129−2136

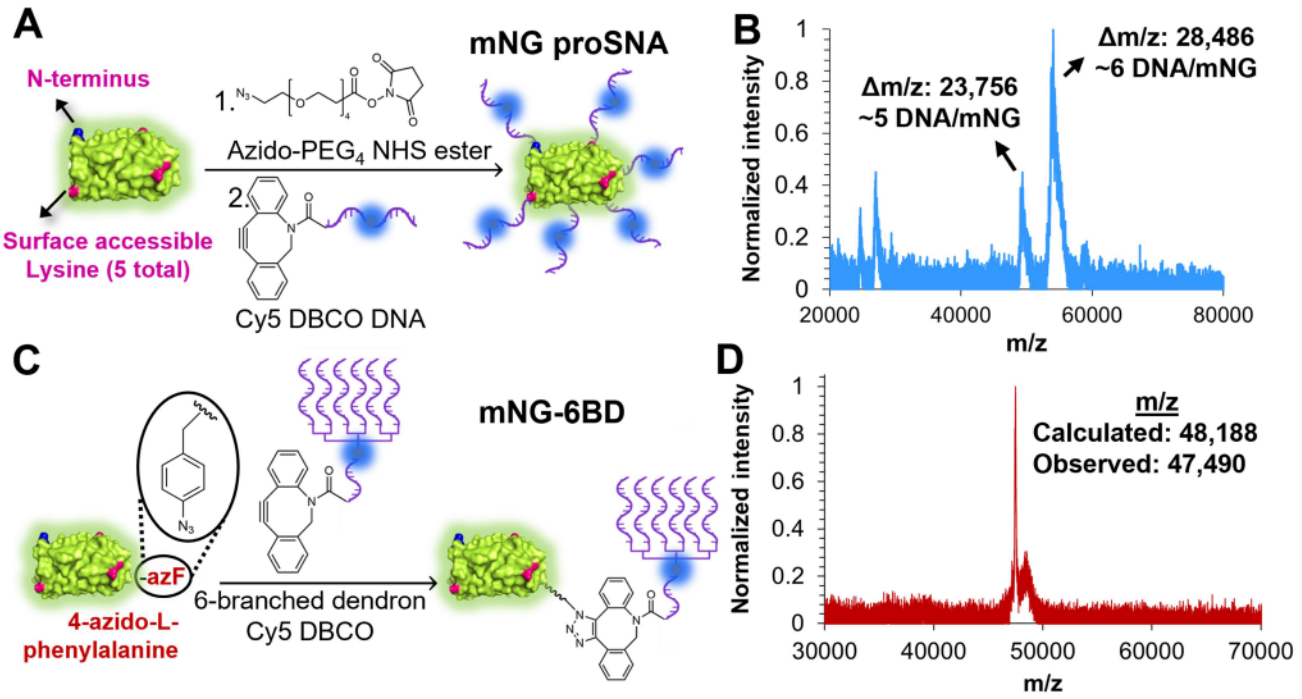

Figure 1. Overview of mNeonGreen (mNG)-DNA construct synthesis and characterization. (A) Synthetic scheme for the mNG proSNA and (B) corresponding MALDI characterization to confirm the synthesis and determine the DNA loading. (C) Six-branched DNA dendron (6BD) is chemically attached to mNG through incorporation of the noncanonical amino acid 4-azido-L-phenylalanine (azF) and (D) corresponding MALDI characterization of the synthesized mNG-6BD construct. (Figures not drawn to scale.).

rapid and enhanced cellular uptake compared to linear DNA, due to their ability to mimic the portion of an SNA that engages with cell surface scavenger receptors.[28,29] This was a significant development as we discovered that a single cluster of DNA is sufficient to achieve SNA-like uptake properties. Furthermore, dendrons can be easily modified to include chemical handles for conjugation to other biological materials and impart SNA-like properties to nanomaterials where conjugating a dense oligonucleotide shell is not always straightforward. We hypothesized that conjugating a DNA dendron onto a protein at even a single attachment point could be a generalizable strategy to enable protein cellular uptake. This novel chemical approach to protein delivery should accelerate the study and application of protein-based constructs for a wide range of intracellular diagnostic and therapeutic applications.

RESULTS AND DISCUSSION

Design and Synthesis of Protein−DNA Constructs. To assess how increasing the local DNA density on a protein surface affects cellular uptake, we chemically modified a fluorescent model protein, mNeonGreen (mNG), with an identical number of DNA strands, either in a radial (proSNA-like) or localized manner (a single DNA dendron). We prioritized using protein mutagenesis for this experiment to ensure precision in number and position of attachment for DNA between both constructs. We chose mNG protein because it can be readily expressed in *Escherichia coli* (*E. coli*) and can tolerate mutagenesis without loss of fluorescent properties.[30] First, we designed different mutants of mNG for the synthesis of mNG proSNA and mNG-dendron (mNG-6BD) to achieve precise DNA loading. The mutant for the proSNA was designed to have a total of six surface accessible amines: five through surface accessible lysine residues (K43, 142, 165, 179, and 200) and one through the N-terminus. The mutant for dendron conjugation was designed to incorporate a single 4-azido-L-phenylalanine (azF) at the C-terminus of the protein (Figure 1A).[31] The mutants were then recombinantly expressed in *E. coli* and purified by Ni-Affinity chromatography.[32] After purification, we obtained the excitation and emission spectra for equal concentrations of the mutants. The data show that the maximum fluorescence of each mutant was nearly identical, allowing for direct comparison of each mutant (Figure S2).

To maintain consistent overall DNA loading density between the mNG proSNA and mNG-6BD, we designed the DNA dendron to have the same number of branches as the maximum number of DNA strands that could be attached to the proSNA. In addition, we matched the length of the DNA shell on the proSNA to the branch length of the DNA dendron (see Table S1 for a list of the oligonucleotides sequences used in this study). As an initial proof-of-concept, we used Cyanine 5 (Cy5) labeled poly-T DNA for this design and synthesized mNG proSNA by modifying the surface accessible primary amines with DNA following established protocols.[16] Briefly, the mNG protein was reacted with azido-polyethylene glycol $(PEG)_4$-*N*-hydroxysuccinimide ester cross-linker (azido-PEG_4 NHS ester) to yield azido-mNG. Then, dibenzocyclooctyne (DBCO)-terminated DNA was reacted with azido-mNG via strain-promoted azide alkyne cycloaddition to yield the mNG proSNA (Figure 1A).[33] We confirmed the success of this reaction via sodium dodecyl sulfate-polyacrylamide gel electrophoresis (SDS-PAGE) (Figure S6) and matrix-assisted laser desorption/ionization time-of-flight mass spectrometry (MALDI) (Figure 1B), which revealed the successful synthesis of mNG proSNAs, with a distribution of proteins with either five or six DNA strands attached. Due to the difficulty in separating the proSNAs with five or six DNA strands, the

https://doi.org/10.1021/jacs.4c16205
J. Am. Chem. Soc. 2025, 147, 2129−2136

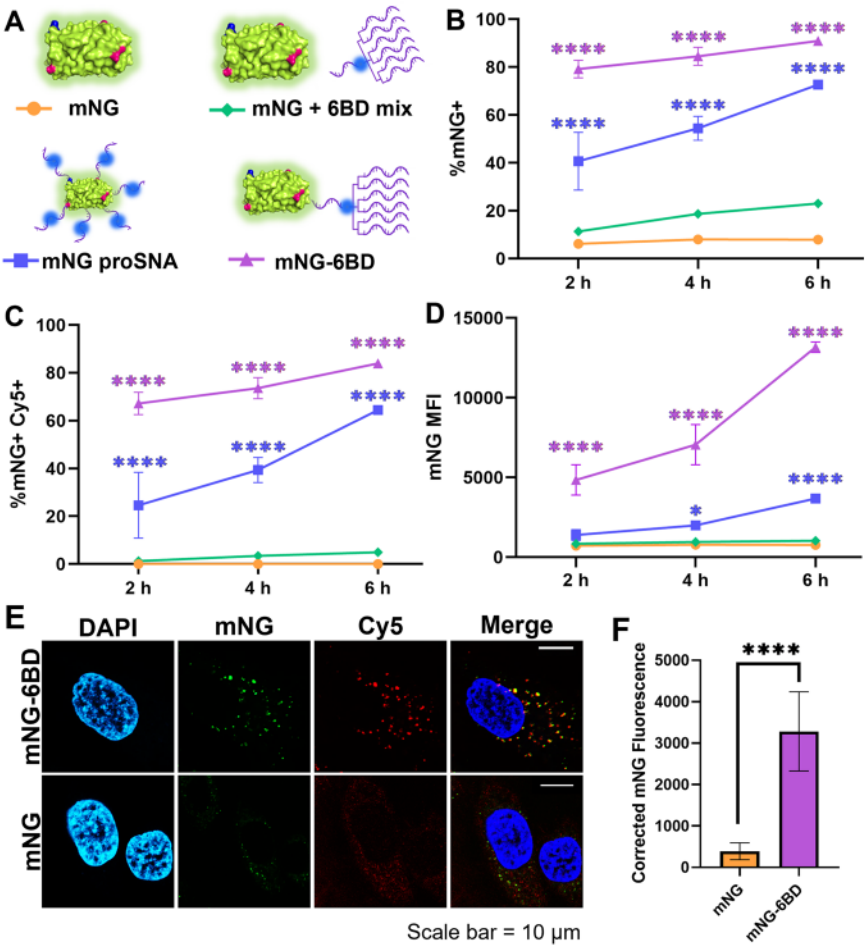

Figure 2. Cellular uptake is enhanced for DNA dendron-protein structures due to localized DNA coverage. The uptake of the mNG constructs (A) was monitored by tracking the mNG and Cy5 (DNA) signals on flow cytometry. The percentage of cells taking up protein (B), protein + DNA (C), and the protein mean fluorescence intensity (MFI) (D) were monitored after treatment of bone marrow-derived dendritic cells (BMDCs) for 2, 4, and 6 h. (E) Representative images for mNG and mNG-6BD uptake after treating HeLa cells with mNG or mNG-6BD for 1 h. Images showing nuclear staining (DAPI), protein (mNG), DNA (Cy5), and merged image from left panel to right, respectively. (F) Quantitative comparison of mNG cellular uptake with confocal microscopy for mNG-6BD and mNG using ImageJ analysis. All data plotted as mean ± standard deviation. Statistics performed in GraphPad Prism using two-way ANOVA for (B–D) and unpaired *t* test for (F) with $*P \leq 0.05$, $****P \leq 0.0001$. Significances in purple for (B–D) indicate significant differences of mNG-6BD treatment compared to all other treatments. Significances in blue for (B–D) indicate significant differences in mNG proSNA treatment compared to the mNG + 6BD mix and mNG treatments. Not all significances are shown for visual clarity.

mixture was utilized in subsequent experiments. We chose a six-branched dendron (6BD) because of its highly efficient uptake into cells.[16] The mNG-6BD construct was synthesized in a single step by reacting the azF on mNG with a DBCO-terminated six-branched dendron via strain promoted azide alkyne cycloaddition (Figure 1C).[33] The success of the reaction was verified with SDS-PAGE (Figure S6) and MALDI (Figure 1D), which revealed a product consistent with the predicted molecular weight. To compare the stability of the proSNA and mNG-6BD structures, an equal concentration of mNG-6BD and mNG proSNA was incubated with 10% fetal bovine serum (FBS) for 1 h or overnight at 37 °C to mimic physiological conditions. Both mNG-6BD and mNG proSNA showed minimal degradation by nucleases (Figure S8), suggesting that both local and radial DNA coverage can provide resistance to nuclease degradation.[34]

Increasing Local DNA Density Enhances Cellular Uptake. Next, we studied how DNA shell design impacts cellular uptake properties. We hypothesized that mNG modified with a single dendron as compared to a proSNA with a similar amount of DNA would exhibit enhanced cellular uptake properties due to the increased local DNA density and its ability to more effectively interact with cell surface scavenger receptors. To test this hypothesis, we treated bone marrow-derived dendritic cells (BMDCs), which are surface-rich in scavenger receptors, with 20 nM mNG, a mixture of mNG and 6BD, mNG proSNA, or mNG-6BD (Figure 2A) and assessed uptake of mNG protein and Cy5 DNA at different time points by flow cytometry. In these experiments, the percentage of uptake represents the percentage of cells that were positive for uptake of protein, DNA, or both compared to the untreated control. A comparison of the mean fluorescence intensities is indicative of the relative uptake per cell, representing the total amount of protein or DNA that has entered cells at a given time.

The data indicate that after 2 h, 80% of the BMDCs had taken up protein when treated with mNG-6BD, compared to just 40% for the mNG proSNA and approximately 10% for mNG treated groups (Figure 2B). This trend was consistent across two additional cell lines, HeLa and JAWSII (Figures S14

https://doi.org/10.1021/jacs.4c16205
J. Am. Chem. Soc. 2025, 147, 2129–2136

and 15) with nearly 100% of the JAWSII cells and >90% of the HeLa cells showing uptake of protein and DNA after 30 min and 2 h of treatment with mNG-6BD, respectively. In contrast, the uptake following treatment with mNG proSNAs remained <50% in both HeLa and JAWSII cell lines at these time points. For each cell line, we observed that the percentage of cells taking up proSNAs steadily increased over time but never reached the same maximum percentage as the mNG-6BD. Furthermore, we demonstrated that the percentage of cells positive for both protein (mNG) and DNA (Cy5) signals was significantly higher in the mNG-6BD treatment group compared to the mNG proSNA and mNG groups at each time point. Notably, at 2 h, this percentage was 65% for mNG-6BD, compared to only 25% for the proSNA (Figure 2C). These data indicate that cells were efficiently internalizing both the protein and DNA in the mNG-6BD treatment groups.

In addition, the mean fluorescence intensity (MFI) from the internalized mNG signal in the BMDC population (Figure 2D) showed that the total amount of protein increased over time for all treatment groups, but the highest rate of increase was observed for mNG-6BD. After 6 h, mNG-6BD showed a 3.5 and 17-fold increase in mNG MFI compared to the mNG proSNA and mNG, respectively. In contrast, the proSNA demonstrated a 4.8-fold increase in MFI compared to mNG. After 6 h treatment in HeLa cells, these enhancements were 2.2 and 6.0-fold compared to the mNG proSNA and mNG, respectively (Figure S15). These results suggest that nearly all cells rapidly take up mNG-6BD and continue to internalize a significant amount of the structure over time. Importantly, mNG-6BD showed no apparent toxicity and had no significant impact on cell viability in BMDCs (Figure S16). Collectively, these results demonstrate that increasing the local DNA density on a protein surface via a single DNA dendron significantly enhances cellular uptake compared to a protein radially functionalized with the same amount of DNA. This finding was consistent across a broad range of cell types where the use of a DNA dendron resulted in an increase in the percentage of cells taking up the conjugate, a higher amount of protein uptake per cell, and enhanced rate of uptake.

To further investigate the uptake of these constructs, we used confocal microscopy to monitor protein and DNA uptake into cells and flow cytometry to examine the mechanism of uptake. We treated HeLa cells with 20 nM of either mNG-6BD or mNG for 1 h and stained them with DAPI to visualize the nuclei. After fixing the cells, we monitored uptake by tracking protein (mNG) and DNA (Cyanine 5) fluorescence. Representative images showed a significantly brighter fluorescence signal for both protein and DNA after treatment with mNG-6BD compared to mNG, indicating efficient uptake of this construct (Figure 2E). Moreover, the mNG and Cy5 DNA signals were largely colocalized, as indicated by the high degree of overlap and higher Mander's colocalization coefficient for mNG-6BD (0.823). To quantify these differences in cellular uptake, the internal fluorescence was measured by calculating the mNG fluorescence intensity inside individual cells upon mNG or mNG-6BD treatment. The data revealed a significantly higher mNG signal for the mNG-6BD treatment group at this time point (Figure 2F). Furthermore, the corrected mean fluorescence of the cells treated with mNG-6BD was significantly higher than that of the mNG treatment group (Figure S19).

Next, to understand the mechanism of internalization of the mNG-6BD construct, we pretreated BMDCs with fucoidan, a scavenger receptor inhibitor, and monitored uptake after a 2 h treatment with either mNG or mNG-6BD.[20,35−39] We hypothesized that the protein-dendron conjugates engage in a similar uptake pathway as dendrons and proSNAs and that inhibiting scavenger-receptor-mediated endocytosis would decrease cellular uptake. Indeed, the data indicate a 60% decrease in the mNG MFI for cells pretreated with fucoidan; this result aligns with the conclusion that these structures undergo scavenger-receptor-mediated endocytosis, which is consistent with what is known about proSNAs (Figure S20).[15] In this experiment, the uptake of mNG-6BD was not completely inhibited, suggesting that this structure likely engages in multiple cellular entry pathways, although scavenger-receptor-A mediated endocytosis is a predominant one.

G-Rich Dendrons Further Enhance Protein Cellular Uptake. To determine whether changes in the structure and sequence of the DNA dendrons influence uptake, we used dendrons with branches composed of G-rich DNA or T-rich DNA. The G-quadruplex structures formed by G-rich DNA have been found to increase cellular uptake due to the natural affinity of the dense G-quadruplexes for the scavenger receptors on cell surfaces. Such G-quadruplex structures are known to form from a tetrad of intramolecular hydrogen bonding interactions between guanine bases around a central metal ion, such as potassium.[40−44] For this experiment, we synthesized a dendron with a poly-T stem and six branches with the $(GGT)_4$ sequence (Table S1). To confirm whether this G-rich dendron could adopt a G-quadruplex secondary structure, we performed circular dichroism spectroscopy in phosphate buffered saline solution (PBS), which is a source of potassium ions necessary for G-quadruplex formation. The T-rich dendrons served as a control in these experiments. In the resulting spectra, the G-rich dendrons exhibited a prominent peak between 250 and 300 nm, consistent with G-quadruplex formation; this peak was absent in the spectrum of the T-rich dendron (Figure S21).[45−47] Then, mNG was conjugated to Cy5-labeled six-branched dendrons containing either a poly T sequence (6BD T12) or $(GGT)_4$ (6BD $(GGT)_4$) as the branch sequence. The T12 branches were chosen such that their length matched that of the branches of the G-rich dendron (for comparing cellular uptake). Then, HeLa cells were treated with 40 nM of mNG, mNG-6BD (T12), or mNG-6BD $(GGT)_4$, and the dendron (Cy5) and protein uptake were monitored by flow cytometry after 2 and 4 h (Figure 3A). These results indicate both dendron branch sequences significantly increase cellular uptake of the construct compared to native protein, as evidenced by the percentage of mNG uptake (Figure S22), mNG MFI (Figure 3B), percent of cells with both mNG and Cy5 (Figure S22), and Cy5 MFI (Figure 3C). However, the G-rich dendron increased the uptake of both protein and DNA at each time point as compared to T-rich dendrons. We observed that the total amount of protein uptake at the 4 h time point increased by 37%, as indicated by the mean fluorescence intensity. In comparison, the largest differences in percentage of uptake were most apparent at the 2 h time point because, after 4 h, nearly all of the cells had internalized both mNG-6BD structures. Consistent with previous reports of SNA uptake properties, these findings show that the sequence of the DNA dendron branches impact uptake[17,40,45] In the future, the impact of other parameters such as additional types of DNA

https://doi.org/10.1021/jacs.4c16205
J. Am. Chem. Soc. 2025, 147, 2129−2136

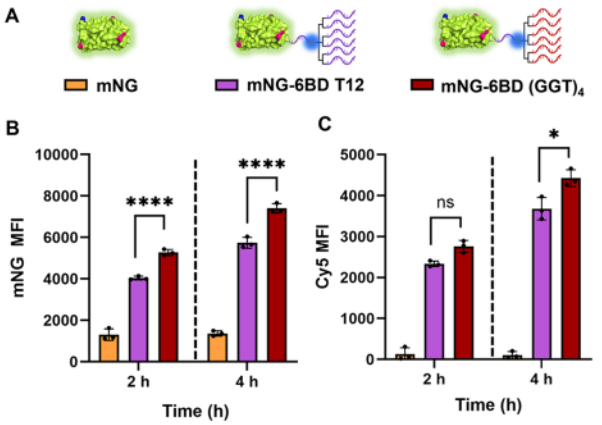

Figure 3. Investigating the effect of dendron sequence on cellular uptake. The effect of dendron sequence on cellular uptake was assessed by treating HeLa cells with mNG or mNG modified with a G-rich dendron or T-rich dendron (A). The cellular uptake of these structures was monitored by flow cytometry through the mean fluorescence intensity (MFI) of mNG (B) and the percentage of cells taking up both mNG and DNA (C). Data from this experiment were obtained in triplicate and plotted as mean ± standard deviation. Statistics: two-way ANOVA performed in GraphPad Prism, $^{**}P \leq 0.01$, $^{****}P \leq 0.0001$. Not all significances are shown for visual clarity.

secondary structures, rigidity, or flexibility, can be investigated for their impact on cellular uptake.

To further investigate the effect of dendron structure on protein uptake, the effect of the length of dendron branches was examined. Accordingly, we synthesized poly-T dendrons with T10, T15, and T20 branch lengths and conjugated them to the azF-containing mNG protein. Interestingly, a proSNA with T20 DNA had significantly enhanced protein and DNA cellular uptake as compared to the proSNAs with T10 and T15 DNA (Figure S23). However, the impact of dendron branch length on uptake was less apparent (Figure S24). Together, these data reveal that localizing DNA through a dendron on a protein surface significantly enhances conjugate cellular uptake compared to a protein with a less dense radial DNA shell. While the dendron branch sequence can be modified to enhance cellular uptake, the length of dendron branches does not significantly affect uptake for the lengths explored here.

Dendrons as a Generalizable Tag for Protein Delivery. We examined the effect of the protein core size on the cellular uptake of protein-dendron conjugates, using proteins of different sizes to evaluate if dendrons can be employed as generalizable tags in nanomedicine. First, we developed a general method for modifying a protein surface with a single dendron but without the need for site-directed mutagenesis. As proof-of-concept, we reacted commercially available bovine serum albumin (BSA) with 10 equiv of azido-polyethylene glycol $(PEG)_4$-*N*-hydroxysuccinimide ester cross-linker and purified it via size-exclusion chromatography to yield azido-BSA. Then, one equivalent of azido-BSA was reacted with one equivalent of a Cy5-labeled DNA dendron terminated with DBCO (6BD T15 Cy5 DBCO, Table S1) via strain-promoted azide alkyne cycloaddition.[33] BSA with a single dendron modification, BSA-6BD, was obtained as the predominant reaction product by controlling the stoichiometry of the dendron to protein in the reaction (Figure S25). The BSA-6BD construct was then further modified with Alexa-Fluor488 succinimidyl ester (AF488) for tracking protein fluorescence (Figure 4A). The final product, a protein with a single dendron, was purified using size-exclusion chromatography and analyzed via SDS-PAGE (Figure S25). The same procedure was applied to two additional proteins, ovalbumin and β-galactosidase (Figures S26 and S27), to verify that this is a viable method for proteins of sizes ranging from 42−464 kDa.

To assess the cellular uptake, HeLa cells were treated with 40 nM AF488-BSA-6BD and AF488-BSA and uptake of the protein and DNA were monitored after 2 and 4 h through AF488 and Cy5 signals, respectively. These results show that adding a single dendron to BSA significantly increased both the percentage of cells taking up protein and the total amount of protein uptake. This is indicated by the increase in percentage of AF488+ cells and the AF488 MFI (Figure 4B,C). This experiment was repeated with the corresponding β-galactosidase and ovalbumin-dendron constructs. The data demonstrate that modification of β-galactosidase with a single DNA dendron significantly enhances the percentage of cells that internalized both protein and DNA, indicated by the increase in cells that contained both AF488 and Cy5 signals compared to native protein (Figure 4D). Furthermore, the modification with a DNA dendron led to a significant increase in the total amount of protein uptake per cell for AF488-βGal-6BD, as demonstrated by the increase in AF488 mean fluorescence intensity at both time points (Figure 4E). Finally, cell treatment with an ovalbumin-dendron construct demonstrated significant cellular uptake of the Cy5 dendron component (Figure S28). Taken together, this work shows that DNA dendrons can serve as tags that facilitate protein delivery for a range of structures, including a small fluorescent protein (mNG, 25 kDa),[30] a structural protein (ovalbumin, 42 kDa),[48] a transport protein (bovine serum albumin, 66 kDa),[49] and a large tetrameric enzyme (β-galactosidase, 464 kDa).[50] This highlights the generalizability of the approach, making it useful for nanomedicine researchers interested in cellular delivery for both therapeutic or diagnostic purposes.

■ CONCLUSIONS

In this study, we demonstrated that tagging proteins with DNA dendrons can enhance cellular internalization. Modifying proteins with clustered DNA dendrons significantly improves cellular uptake compared to proteins with a less dense radial coverage of DNA. Our data indicate that over 90% of cells internalize proteins tagged with DNA dendrons within 30 min, achieving up to an 8-fold increase in total protein uptake relative to proteins with sparser DNA coverage at the same time point. This finding suggests that clustering oligonucleotides on a protein surface effectively facilitates cellular uptake and may provide advantages over traditional methods that uniformly modify the entire protein surface. Such an approach reduces the risk of chemical denaturation of the protein. Additionally, the DNA sequences within the dendrons can be customized to further enhance uptake, with G-rich dendrons showing higher cellular uptake than T-rich dendrons. This is attributed to the formation of G-quadruplex structures, characterized by tetrads of hydrogen bonds between guanine bases, which are recognized and bound by scavenger receptors that facilitate uptake.[40−44] We have also developed a straightforward method for creating dendron-protein nanomaterials without the need for mutagenesis, achieving up to a 17-fold increase in cellular uptake across a variety of protein sizes (ranging from 42 to 464 kDa) and functions. This novel

https://doi.org/10.1021/jacs.4c16205
J. Am. Chem. Soc. 2025, 147, 2129−2136

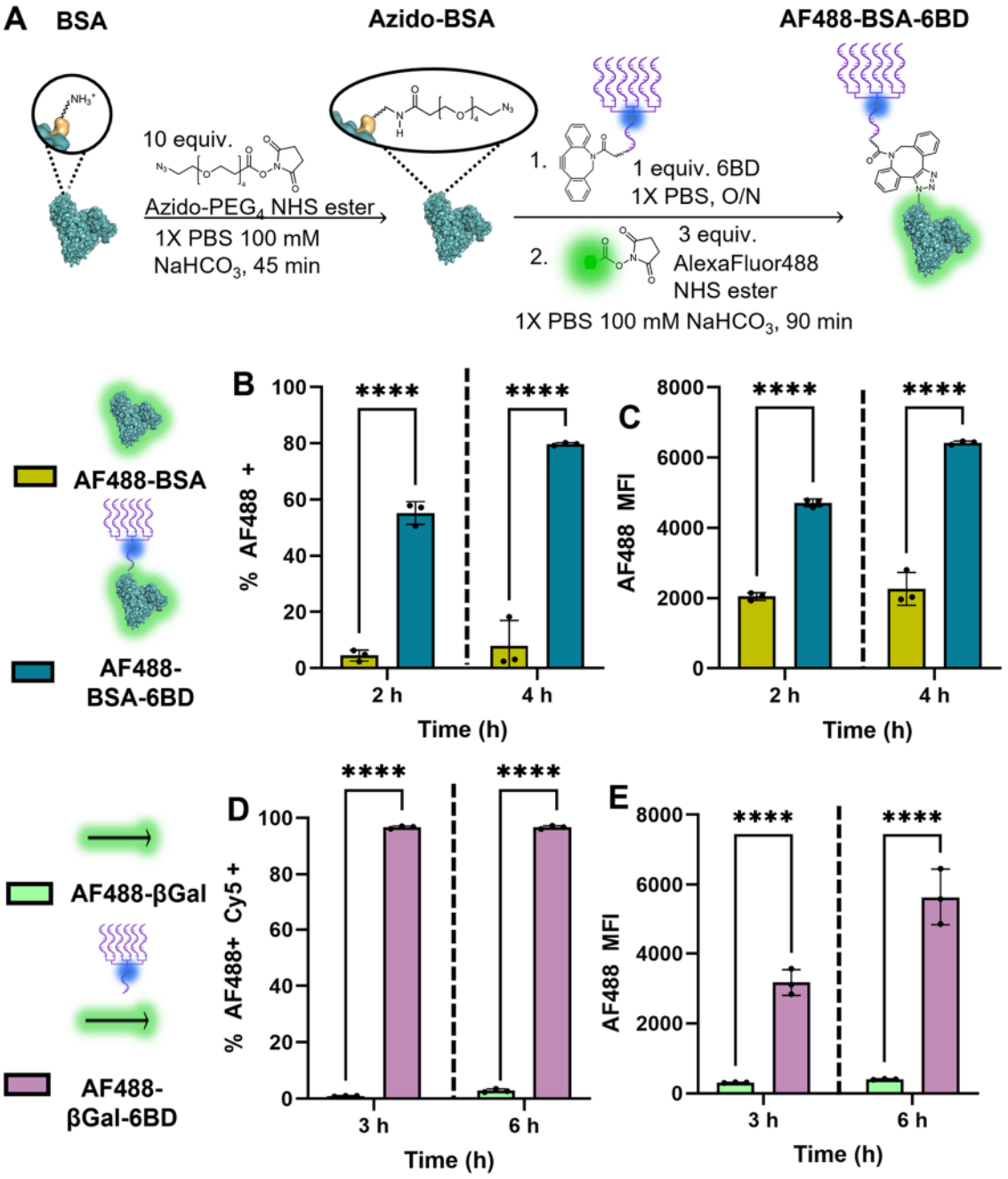

Figure 4. DNA dendron tags as a generalizable intracellular protein delivery agent. (A) Generalizable strategy for modifying BSA, a model protein, with a single dendron that does not require mutagenesis. The cellular uptake properties of BSA and β-galactosidase after modification with the DNA dendron were investigated in HeLa cells. For BSA, the cellular uptake was monitored as a function of percentage of cells taking up protein (B) and amount of protein uptake (C). For β-galactosidase, uptake was monitored through the percentage of cells containing both AF488 and Cy5 (D) and total amount of protein uptake (E). Data obtained in triplicate and plotted as mean $\pm$ standard deviation. Statistics: 2-way ANOVA performed in GraphPad Prism. ****$P \leq 0.0001$.

strategy holds great potential for advancing the development and application of protein-based therapeutics and diagnostic tools.

■ ASSOCIATED CONTENT

Supporting Information

The Supporting Information is available free of charge at https://pubs.acs.org/doi/10.1021/jacs.4c16205.

Oligonucleotide sequences, experimental methods, flow cytometry gating, and additional experiments (PDF)

■ AUTHOR INFORMATION

Corresponding Author

Chad A. Mirkin − *Department of Chemistry and International Institute for Nanotechnology, Northwestern University, Evanston, Illinois 60208, United States;* orcid.org/0000-0002-6634-7627; Email: chadnano@northwestern.edu

Authors

Kathleen H. Ngo − *Department of Chemistry and International Institute for Nanotechnology, Northwestern*

https://doi.org/10.1021/jacs.4c16205
J. Am. Chem. Soc. 2025, 147, 2129−2136

University, Evanston, Illinois 60208, United States; orcid.org/0009-0000-0626-1509

Max E. Distler – *Department of Chemistry and International Institute for Nanotechnology, Northwestern University, Evanston, Illinois 60208, United States;* orcid.org/0000-0002-3750-5075

Michael Evangelopoulos – *Department of Biomedical Engineering and International Institute for Nanotechnology, Northwestern University, Evanston, Illinois 60208, United States;* orcid.org/0000-0002-5300-4289

Tonatiuh A. Ocampo – *Interdisciplinary Biological Sciences Graduate Program and International Institute for Nanotechnology, Northwestern University, Evanston, Illinois 60208, United States*

Yinglun Ma – *Department of Chemistry and International Institute for Nanotechnology, Northwestern University, Evanston, Illinois 60208, United States;* orcid.org/0000-0002-1788-0353

Andrew J. Minorik – *Department of Neurobiology, Northwestern University, Evanston, Illinois 60208, United States*

Complete contact information is available at: https://pubs.acs.org/10.1021/jacs.4c16205

Notes

The authors declare the following competing financial interest(s): C.A.M. has financial interests in Flashpoint Therapeutics which could potentially benefit from the outcomes of this research.

■ ACKNOWLEDGMENTS

Research reported in this publication was supported by the National Cancer Institute of the National Institutes of Health awards R01CA257926 and R01CA275430, and the National Institute of Diabetes and Digestive and Kidney Diseases of the National Institutes of Health award U54DK137516. The content is solely the responsibility of the authors and does not necessarily represent the official views of the National Institutes of Health. This material is also based upon work supported by the National Science Foundation grant DMR-2428112. M.E. was partially supported by the Dr. John N. Nicholson Fellowship and the Alexander S. Onasis Public Benefit Foundation. Molecular graphics and analyses performed with UCSF Chimera, developed by the Resource for Biocomputing, Visualization, and Informatics at the University of California, San Francisco, with support from NIH P41-GM103311.

■ REFERENCES

(1) Dimitrov, D. S. Therapeutic Proteins. *Methods Mol. Biol.* **2012**, *899*, 1–26.

(2) Leader, B.; Baca, Q.; Golan, D. E. Protein Therapeutics: A Summary and Pharmacological Classification. *Nat. Rev. Drug. Discovery* **2008**, *7*, 21–39.

(3) Ebrahimi, S. B.; Samanta, D. Engineering Protein-Based Therapeutics through Structural and Chemical Design. *Nat. Commun.* **2023**, *14*, 2411.

(4) Fu, A.; Tang, R.; Hardie, J.; Farkas, M. E.; Rotello, V. M. Promises and Pitfalls of Intracellular Delivery of Proteins. *Bioconjugate Chem.* **2014**, *25* (9), 1602–1608.

(5) Tian, Y.; Tirrell, M. V.; LaBelle, J. L. Harnessing the Therapeutic Potential of Biomacromolecules through Intracellular Delivery of Nucleic Acids, Peptides, and Proteins. *Adv. Healthc. Mater.* **2022**, *11* (12), No. e2102600.

(6) Kintzing, J. R.; Filsinger Interrante, M. V.; Cochran, J. R. Emerging Strategies for Developing Next-Generation Protein Therapeutics for Cancer Treatment. *Trends Pharmacol. Sci.* **2016**, *37* (12), 993–1008.

(7) Carter, P. J. Introduction to Current and Future Protein Therapeutics: A Protein Engineering Perspective. *Exp. Cell Res.* **2011**, *317* (9), 1261–1269.

(8) Kariolis, M. S.; Kapur, S.; Cochran, J. R. Beyond Antibodies: Using Biological Principles to Guide the Development of next-Generation Protein Therapeutics. *Curr. Opin. Biotechnol.* **2013**, *24* (6), 1072–1077.

(9) Xie, J.; Bi, Y.; Zhang, H.; Dong, S.; Teng, L.; Lee, R. J.; Yang, Z. Cell-Penetrating Peptides in Diagnosis and Treatment of Human Diseases: From Preclinical Research to Clinical Application. *Front. Pharmacol.* **2020**, *11*, 697.

(10) Kim, G. C.; Cheon, D. H.; Lee, Y. Challenge to Overcome Current Limitations of Cell-Penetrating Peptides. *Biochim. Biophys. Acta Proteins Proteom.* **2021**, *1869* (4), No. 140604.

(11) Zorko, M.; Jones, S.; Langel, Ü. Cell-Penetrating Peptides in Protein Mimicry and Cancer Therapeutics. *Adv. Drug Deliv. Rev.* **2022**, *180*, No. 114044.

(12) Copolovici, D. M.; Langel, K.; Eriste, E.; Langel, Ü. Cell-Penetrating Peptides: Design, Synthesis, and Applications. *ACS Nano* **2014**, *8* (3), 1972–1994.

(13) Zhang, H.; Zhang, Y.; Zhang, C.; Yu, H.; Ma, Y.; Li, Z.; Shi, N. Recent Advances of Cell-Penetrating Peptides and Their Application as Vectors for Delivery of Peptide and Protein-Based Cargo Molecules. *Pharmaceutics* **2023**, *15* (8), 2093.

(14) Bottens, R. A.; Yamada, T. Cell-Penetrating Peptides (CPPs) as Therapeutic and Diagnostic Agents for Cancer. *Cancers* **2022**, *14* (22), 5546.

(15) Brodin, J. D.; Sprangers, A. J.; Mcmillan, J. R.; Mirkin, C. A. DNA-Mediated Cellular Delivery of Functional Enzymes. *J. Am. Chem. Soc.* **2015**, *137*, 14838–14841.

(16) Ebrahimi, S. B.; Samanta, D.; Kusmierz, C. D.; Mirkin, C. A. Protein Transfection via Spherical Nucleic Acids. *Nat. Protoc.* **2022**, *17*, 327–357.

(17) Kusmierz, C. D.; Bujold, K. E.; Callmann, C. E.; Mirkin, C. A. Defining the Design Parameters for in Vivo Enzyme Delivery through Protein Spherical Nucleic Acids. *ACS Cent. Sci.* **2020**, *6* (5), 815–822.

(18) Samanta, D.; Ebrahimi, S. B.; Kusmierz, C. D.; Cheng, H. F.; Mirkin, C. A. Protein Spherical Nucleic Acids for Live-Cell Chemical Analysis. *J. Am. Chem. Soc.* **2020**, *142*, 13350–13355.

(19) Huang, C.; Han, Z.; Evangelopoulos, M.; Mirkin, C. A. CRISPR Spherical Nucleic Acids. *J. Am. Chem. Soc.* **2022**, *144* (41), 18756–18760.

(20) Choi, C. H. J.; Hao, L.; Narayan, S. P.; Auyeung, E.; Mirkin, C. A. Mechanism for the Endocytosis of Spherical Nucleic Acid Nanoparticle Conjugates. *Proc. Natl. Acad. Sci. U. S. A.* **2013**, *110* (19), 7625–7630.

(21) Patel, P. C.; Giljohann, D. A.; Daniel, W. L.; Zheng, D.; Prigodich, A. E.; Mirkin, C. A. Scavenger Receptors Mediate Cellular Uptake of Polyvalent Oligonucleotide-Functionalized Gold Nanoparticles. *Bioconjugate Chem.* **2010**, *21* (12), 2250–2256.

(22) Taban, Q.; Mumtaz, P. T.; Masoodi, K. Z.; Haq, E.; Ahmad, S. M. Scavenger Receptors in Host Defense: From Functional Aspects to Mode of Action. *Cell Commun. Signal.* **2022**, *20* (1), 2.

(23) Alquraini, A.; El Khoury, J. Scavenger Receptors. *Curr. Biol.* **2020**, *30* (14), R790–R795.

(24) Canton, J.; Neculai, D.; Grinstein, S. Scavenger Receptors in Homeostasis and Immunity. *Nat. Rev. Immunol.* **2013**, *13* (9), 621–634.

(25) Giljohann, D. A.; Seferos, D. S.; Patel, P. C.; Millstone, J. E.; Rosi, N. L.; Mirkin, C. A. Oligonucleotide Loading Determines Cellular Uptake of DNA-Modified Gold Nanoparticles. *Nano Lett.* **2007**, *7* (12), 3818–3821.

(26) Hurst, S. J.; Lytton-Jean, A. K. R.; Mirkin, C. A. Maximizing DNA Loading on a Range of Gold Nanoparticle Sizes. *Anal. Chem.* **2006**, *78* (24), 8313–8318.

(27) Li, H.; Zhang, B.; Lu, X.; Tan, X.; Jia, F.; Xiao, Y.; Cheng, Z.; Li, Y.; Silva, D. O.; Schrekker, H. S.; Zhang, K.; Mirkin, C. A. Molecular Spherical Nucleic Acids. *Proc. Natl. Acad. Sci. U. S. A.* **2018**, *115* (17), 4340−4344.
(28) Distler, M. E.; Teplensky, M. H.; Bujold, K. E.; Kusmierz, C. D.; Evangelopoulos, M.; Mirkin, C. A. DNA Dendrons as Agents for Intracellular Delivery. *J. Am. Chem. Soc.* **2021**, *143* (34), 13513−13518.
(29) Distler, M. E.; Cavaliere, J. P.; Teplensky, M. H.; Evangelopoulos, M.; Mirkin, C. A. Molecular DNA Dendron Vaccines. *Proc. Natl. Acad. Sci. U. S. A.* **2023**, *120* (5), No. e2215091120.
(30) Clavel, D.; Gotthard, G.; Von Stetten, D.; De Sanctis, D.; Ne Pasquier, H.; Lambert, G. G.; Shaner, N. C.; Royant, A. Structural Analysis of the Bright Monomeric Yellow-Green Fluorescent Protein MNeonGreen Obtained by Directed Evolution. *Acta Crystallogr.* **2016**, *72*, 1298−1307.
(31) Wang, Y.; Zhang, J.; Han, B.; Tan, L.; Cai, W.; Li, Y.; Su, Y.; Yu, Y.; Wang, X.; Duan, X.; Wang, H.; Shi, X.; Wang, J.; Yang, X.; Liu, T. Noncanonical Amino Acids as Doubly Bio-Orthogonal Handles for One-Pot Preparation of Protein Multiconjugates. *Nat. Commun.* **2023**, *14* (1), 974.
(32) Raran-Kurussi, S.; Waugh, D. S. In. *Methods Mol. Biol.* **2017**, *1607*, 1−15.
(33) Agard, N. J.; Prescher, J. A.; Bertozzi, C. R. A Strain-Promoted [3 + 2] Azide-Alkyne Cycloaddition for Covalent Modification of Biomolecules in Living Systems. *J. Am. Chem. Soc.* **2004**, *126*, 15046−15047.
(34) Seferos, D. S.; Prigodich, A. E.; Giljohann, D. A.; Patel, P. C.; Mirkin, C. A. Polyvalent DNA Nanoparticle Conjugates Stabilize Nucleic Acids. *Nano Lett.* **2009**, *9* (1), 308−311.
(35) Lin, Z.; Tan, X.; Zhang, Y.; Li, F.; Luo, P.; Liu, H. Molecular Targets and Related Biologic Activities of Fucoidan: A Review. *Mar. Drugs* **2020**, *18* (8), 376.
(36) Peiser, L.; Gordon, S. The Function of Scavenger Receptorsexpressed by Macrophages and Their Rolein the Regulation of Inflammation. *Microbes Infect.* **2001**, *3* (2), 149−159.
(37) Wang, R.; Chandawarkar, R. Y. Phagocytosis of Fungal Agents and Yeast via Macrophage Cell Surface Scavenger Receptors. *J. Surg. Res.* **2010**, *164* (2), 273−279.
(38) Thelen, T.; Hao, Y.; Medeiros, A. I.; Curtis, J. L.; Serezani, C. H.; Kobzik, L.; Harris, L. H.; Aronoff, D. M. The Class A Scavenger Receptor, Macrophage Receptor with Collagenous Structure, Is the Major Phagocytic Receptor for Clostridium Sordellii Expressed by Human Decidual Macrophages. *J. Immunol.* **2010**, *185* (7), 4328−4335.
(39) Obrien, D. K.; Correspondence, S. B. M; Melville, S. B. Multiple Effects on Clostridium Perfringens Binding, Uptake and Trafficking to Lysosomes by Inhibitors of Macrophage Phagocytosis Receptors. *Microbiology* **2003**, *149* (6), 1377−1386.
(40) Chinen, A. B.; Guan, C. M.; Mirkin, C. A. Spherical Nucleic Acid Nanoparticle Conjugates Enhance G-Quadruplex Formation and Increase Serum Protein Interactions. *Angew. Chemie Int. Ed.* **2015**, *54* (2), 527−531.
(41) Narayan, S. P.; Choi, C. H. J.; Hao, L.; Calabrese, C. M.; Auyeung, E.; Zhang, C.; Goor, O. J. G. M.; Mirkin, C. A. The Sequence-Specific Cellular Uptake of Spherical Nucleic Acid Nanoparticle Conjugates. *Small.* **2015**, *11* (33), 4173−4182.
(42) Pearson, A. M.; Rich, A.; Krieger, M. Polynucleotide Binding to Macrophage Scavenger Receptors Depends on the Formation of Base-Quartet-Stabilized Four-Stranded Helices. *J. Biol. Chem.* **1993**, *268* (5), 3546−3554.
(43) Sen, D.; Gilbert, W. Formation of Parallel Four-Stranded Complexes by Guanine-Rich Motifs in DNA and Its Implications for Meiosis. *Nature.* **1988**, *334* (6180), 364−366.
(44) Burge, S.; Parkinson, G. N.; Hazel, P.; Todd, A. K.; Neidle, S. Quadruplex DNA: Sequence, Topology and Structure. *Nucleic Acids Res.* **2006**, *34* (19), 5402−5415.
(45) del Villar-Guerra, R.; Trent, J. O.; Chaires, J. B. G-Quadruplex Secondary Structure Obtained from Circular Dichroism Spectroscopy. *Angew. Chemie Int. Ed.* **2018**, *57* (24), 7171−7175.
(46) Del Villar-Guerra, R.; Gray, R. D.; Chaires, J. B. Characterization of Quadruplex DNA Structure by Circular Dichroism. *Curr. Protoc. Nucleic Acid Chem.* **2017**, *68* (1), 17.8.1−17.8.16.
(47) Randazzo, A.; Spada, G. P.; da Silva, M. W. Circular Dichroism of Quadruplex Structures. *Top. Curr. Chem.* **2012**, *330*, 67−86.
(48) Razi, S. M.; Fahim, H.; Amirabadi, S.; Rashidinejad, A. An Overview of the Functional Properties of Egg White Proteins and Their Application in the Food Industry. *Food Hydrocoll.* **2023**, *135* (4), No. 108183.
(49) Majorek, K. A.; Porebski, P. J.; Dayal, A.; Zimmerman, M. D.; Jablonska, K.; Stewart, A. J.; Chruszcz, M.; Minor, W. Structural and Immunologic Characterization of Bovine, Horse, and Rabbit Serum Albumins. *Mol. Immunol.* **2012**, *52* (3−4), 174−182.
(50) Juers, D. H.; Matthews, B. W.; Huber, R. E. LacZ β-Galactosidase: Structure and Function of an Enzyme of Historical and Molecular Biological Importance. *Protein Sci.* **2012**, *21* (12), 1792−1807.

https://doi.org/10.1021/jacs.4c16205
J. Am. Chem. Soc. 2025, 147, 2129−2136